# Infrared Spectra and Density Functional Theory Calculations of Group 4 Transition Metal Sulfides

**Binyong Liang and Lester Andrews***

*Department of Chemistry, University of Virginia, P.O. Box 400319, Charlottesville, Virginia 22904-4319*

*Received: January 23, 2002; In Final Form: May 3, 2002*

Laser-ablated titanium, zirconium, and hafnium atoms react with discharged sulfur vapor during co-condensation in excess argon. The primary reaction product $MS_2$ molecules are identified for the first time, and evidence for metal monosulfides is also presented. The $\nu_1$ and $\nu_3$ modes for $TiS_2$, $ZrS_2$, and $HfS_2$ absorb at 533.5 and 577.8 $cm^{-1}$, 502.9 and 504.6 $cm^{-1}$, and 492.2 and 483.2 $cm^{-1}$, respectively, in solid argon. On the basis of the isotopic frequencies for the $\nu_3$ modes, the bond angles of $TiS_2$, $ZrS_2$, and $HfS_2$ are determined as 113 ± 4°, 107 ± 4°, and 108 ± 4°. DFT/B3LYP calculations predict $^1A_1$ ground states and bond angles of 113.3°, 108.5°, and 109.5°, for the $MS_2$ molecules, M = Ti, Zr, and Hf, respectively, and frequencies in excellent agreement with the observed values. The same calculation also predicts $^3\Delta$ ground states for TiS and ZrS, the $^1\Sigma^+$ ground state for HfS, and frequencies in agreement with the observed values.

## I. Introduction

Transition metal sulfur compounds are important for both biochemical and industrial catalysis.[1,2] Solid transition metal sulfides have been used as hydrodesulfurization catalysts.[3] In addition, titanium sulfide complexes have been employed for dihydrogen activation.[4] Transition metal sulfides are also involved in other areas of research, for example, in astrophysics, as lines of TiS and ZrS have been found in the spectra of S-type stars,[5] and in synthetic chemistry as novel binary titanium(IV) sulfides have been prepared.[6]

Emission spectra for all three metal monosulfides in the gas phase have been observed. First TiS was reported by Clements and Barrow[7] and later by two different groups,[8−10] and the ground state was determined as $^3\Delta$. Since the first laboratory study on ZrS,[11] both the singlet and triplet spectra have been investigated in detail[12−14] along with spectroscopic studies on HfS.[15,16] Both ZrS and HfS reportedly possess the $^1\Sigma^+$ ground states, and a microwave spectroscopic study reinforced the $^1\Sigma^+$ ground state for ZrS.[17] In addition, the transient frequency modulation absorption spectrum of TiS was reported,[18] and permanent electric dipole moments of TiS and ZrS were determined using the Stark measurements.[19] An earlier argon matrix study reacting transition metal atoms and OCS reported the vibration of TiS.[20] Theoretical calculations predicted the $^3\Delta$ ground state for TiS,[21] and the $^1\Sigma^+$ ground state for ZrS, but the $^3\Delta$ state is only 209 $cm^{-1}$ higher.[22] Finally, cationic metal sulfides have been studied by two different groups using mass spectroscopic techniques.[23,24]

To our knowledge, neither experimental nor theoretical studies have been performed for the metal disulfide molecules. In light of detailed studies of the diatomic metal oxides and sulfides,[21] it will be interesting to compare the group 4 dioxide and disulfide molecular properties. We report here a combined matrix IR and density functional theory (DFT) investigations of group 4 sulfides and show that agreement between the two is excellent, which underscores the predictive power of DFT frequency and structure calculations.

* Author to whom correspondence should be addressed.

## II. Experimental and Computational Methods

Sulfur atoms and small molecules were generated by a microwave discharge in argon seeded with sulfur vapor. The coaxial quartz discharge tube is similar to the one used in the earlier experiments.[25] Natural isotopic sulfur (Electronic Space Products, Inc., recrystallized) and enriched sulfur (98% $^{34}S$, EG&G Mound Applied Technologies) were used as received: different mixtures of the two isotopic samples were also employed. The vapor pressure of sulfur located in the sidearm was controlled by the resistively heated windings. The microwave discharge was sustained in the argon−sulfur mixture by an Opthos Instruments 120 W microwave discharge (operated at 30−50% of the maximum power level) with a Evenson-Broida cavity and extended from a region about 5 cm downstream of the sulfur reservoir to the end of the discharge tube. The presence of significant quantities of $S_2$ in the discharge was indicated by the sky-blue emission,[26,27] which is different from the normal pink argon discharge.

The experimental method for laser ablation and matrix isolation has been described in detail previously.[28,29] Briefly, the Nd:YAG laser fundamental (1064 nm, 10 Hz repetition rate with 10 ns pulse width, 3−5 mJ/pulse) was focused to ablate the rotating titanium (Goodfellow Metals, 99.6%), zirconium, or hafnium (Johnson-Matthey) metal target. Laser-ablated metal atoms were co-deposited with a sulfur-doped spray-on argon stream onto a 7 K CsI cryogenic window at 2−4 mmol/h for 0.5−1.5 h. Infrared spectra were recorded at 0.5 $cm^{-1}$ resolution on a Nicolet 550 spectrometer with 0.1 $cm^{-1}$ accuracy using a mercury cadmium telluride detector down to 400 $cm^{-1}$. Matrix samples were annealed at different temperatures, and selected samples were subjected to irradiation using a medium-pressure mercury lamp ($\lambda$ > 240 nm) with the globe removed.

DFT calculations were performed on all proposed metal sulfides using the GAUSSIAN 98 program[30] and the B3LYP[31] functional. Additional calculations with the BPW91[32] functional or second-order Møller−Plesset (MP2) method[33] were performed on ZrS. The 6-311+G* basis set was used for sulfur and titanium,[34] and the LanL2DZ effective core potential and

10.1021/jp0202183 CCC: $22.00 
Published on Web 06/12/2002

**TABLE 1: Infrared Absorptions (cm$^{-1}$) from Codeposition of Laser-Ablated Ti, Zr, and Hf Atoms with Discharged Sulfur in Excess Argon**

| $^{32}$S | $^{34}$S | $^{32}$S + $^{34}$S | *R*(32/34) | identity |
|---|---|---|---|---|
| | | Titanium | | |
| 583.8 | 575.2 | | 1.0150 | $^{46}TiS_2$ site A, $\nu_3$ |
| 580.6 | 571.9 | | 1.0152 | $^{47}TiS_2$ site A, $\nu_3$ |
| 577.8 | 569.1 | 577.8, 574.0, 569.1 | 1.0153 | $^{48}TiS_2$ site A, $\nu_3$ |
| 571.4 | 562.6 | 571.4, 567.6, 562.6 | 1.0156 | $^{48}TiS_2$ site B, $\nu_3$ |
| 566.0 | 557.1 | | 1.0160 | $^{50}TiS_2$ site B, $\nu_3$ |
| 557.6 | 547.6 | | 1.0183 | TiS? |
| 539.2 | 529.7 | | 1.0179 | $Ti_xS$ |
| 533.5 | 522.8 | | 1.0205 | $^{48}TiS_2$ site A, $\nu_1$ |
| 528.3 | 517.8 | 528.3, 522.7, 517.9 | 1.0203 | $^{48}TiS_2$ site B, $\nu_1$ |
| | | Zirconium | | |
| 518.1 | 506.8 | 518.1, 506.8 | 1.0221 | ZrS |
| 504.6 | 494.5 | 504.6, 503.8, 494.5 | 1.0204 | $^{90}ZrS_2$, $\nu_3$ |
| 502.9 | 492.8 | | 1.0205 | $^{92}ZrS_2$, $\nu_3$ |
| 502.9 | 491.0 | 502.9, 492.7, 491.0 | 1.0242 | $^{90}ZrS_2$, $\nu_1$ |
| 501.3 | | | | $^{94}ZrS_2$, $\nu_3$ |
| | | Hafnium | | |
| 520.3 | 507.1 | 520.3, 507.3 | 1.0260 | HfS |
| 497.2 | 484.6 | 497.2, 484.6 | 1.0260 | $(S_2)$HfS |
| 492.2 | 479.2 | 492.2, 488.9, 479.2 | 1.0271 | $HfS_2$, $\nu_1$ |
| 483.2 | 471.6 | 483.2, 474.2, 471.7 | 1.0246 | $HfS_2$, $\nu_3$ |
| 471.1 | 458.1 | 471.1, 464.8, 458.1 | 1.0284 | $(S_2)$HfS |

basis set was employed for zirconium and hafnium[35] since these standard basis sets worked well for recent group 5 transition metal sulfide calculations.[36]

## III. Results

**Infrared Spectra.** Figures 1−6 show selected regions in the infrared spectra of samples produced by reactions between laser-ablated Ti, Zr, or Hf atoms and discharged isotopic sulfur/argon mixtures. The metal related infrared absorptions are listed in Table 1, along with their proposed assignments. Complementary experiments were done with laser-ablated titanium and an Ar/OCS sample. The behaviors of product bands in different experiments and their assignments will be discussed in the next section. Besides these listed product bands, common absorptions observed in all three metal experiments include $S_3$ at 679.8 and 676.0 cm$^{-1}$, $S_4$ at 661.7 and 642.4 cm$^{-1}$, $CS_2$ at 1528.0 cm$^{-1}$, and weak $S_2O$ at 1157.1 cm$^{-1}$. These bands have been reported earlier,[25] and will not be discussed in this paper.

**DFT Calculations.** The ground-state configurations of S, Ti, Zr, and Hf atoms were reproduced as [Ne]3s$^2$3p$^4$, [Ar]3d$^2$4s$^2$, [Kr]4d$^2$5s$^2$, and [Xe]4f$^{14}$5d$^2$6s$^2$, respectively. The calculations on $S_2$ and $S_3$ found ground states of $^3\Sigma_g^-$ and $^1A_1$, respectively. The S−S bond length in the $S_2$ molecule is predicted as 1.927 Å, whereas in the $S_3$ molecule, the S−S bond length is computed as 1.952 Å, and the bond angle as 118.2°. For comparison, valance angle calculations from four pairs of symmetrical isotopic $\nu_3$ values gave 116 ± 2° for $S_3$.[25] Calculations for metal sulfides were performed on different spin states, with different starting geometries. We switched occupied and virtual orbitals to confirm that the state under consideration was in fact the ground state. Analytical second-derivatives were used to obtain the harmonic frequencies. For both TiS and ZrS, the ground states are $^3\Delta$ ($\delta^1\sigma^1$), whereas HfS has the ground state of $^1\Sigma^+$ ($\sigma^2$). These results agree with previous observations except for ZrS,[17] where the reported ground state is $^1\Sigma^+$. This discrepancy will be addressed in the next section. For metal disulfides, the ground states are $^1A_1$ in $C_{2v}$ symmetry. The results of group 4 sulfide calculations are summarized in Tables 2, 3, and 4.

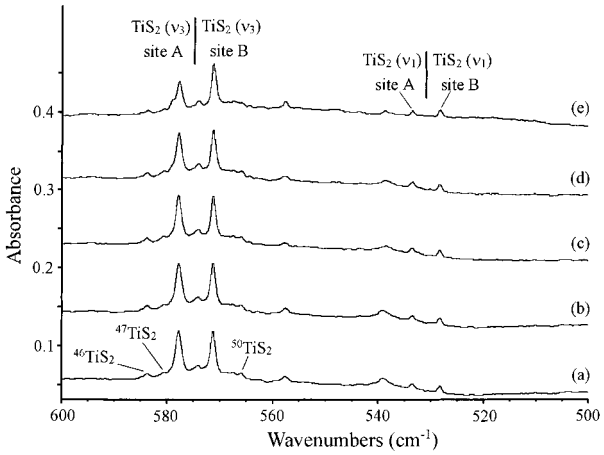


**Figure 1.** Infrared spectra in the 600−500 cm$^{-1}$ region for laser-ablated Ti co-deposited with discharged S in argon at 7 K. (a) sample deposited for 50 min, (b) after 25 K annealing, (c) after $\lambda$ > 240 nm irradiation, (d) after 35 K annealing, (e) after 40 K annealing.

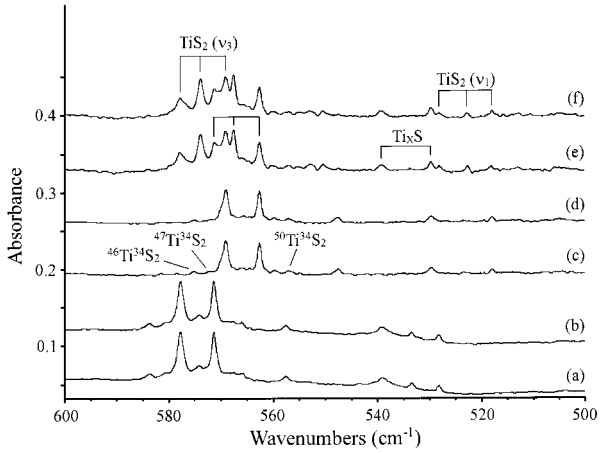


**Figure 2.** Infrared spectra in the 600−500 cm$^{-1}$ region for laser-ablated Ti co-deposited with discharged S in argon at 7 K. (a, b) $^{32}$S, (c, d) $^{34}$S, (e, f) 50/50 $^{32}$S + $^{34}$S mixture. Spectra (a, c, e) are collected after sample deposition, and spectra (b, d, f) after 25 K annealing.

## IV. Discussion

Group 4 transition metal sulfide infrared spectra will be assigned in turn.

**$MS_2$ (M = Ti, Zr, Hf).** *$TiS_2$.* The reaction between laser-ablated Ti atoms and sulfur produced two strong absorptions at 571.4 and 577.8 cm$^{-1}$ on deposition (Figure 1a). These two bands showed little change on subsequent annealing and ultraviolet irradiation. In the $^{34}$S-substituted sample, counterparts were observed at 562.6 and 569.1 cm$^{-1}$ with $^{32}$S/$^{34}$S isotopic frequency ratios of 1.0156 and 1.0153. In the mixed $^{32}$S + $^{34}$S experiments (Figure 2e,f), both bands clearly split into triplets with intermediate bands at 567.6 and 574.0 cm$^{-1}$, respectively. The triplet splitting pattern demonstrates that two equivalent sulfur atoms are involved in this vibrational mode, and these two bands are assigned to the antisymmetric S−Ti−S stretching mode in the $TiS_2$ molecule at two different argon matrix sites (labeled as site A, site B in Figure 1). The involvement of only one Ti atom in this molecule is confirmed by the metal isotopic splitting pattern, where the relative absorption intensities for these bands are in accord with the natural-abundance pattern for a single titanium atom.[37] The lighter $^{46}TiS_2$ and $^{47}TiS_2$ isotopic molecules were observed for the $^{48}TiS_2$ site A and the heavier $^{50}TiS_2$ molecule for site B. The corresponding symmetric S−Ti−S stretching mode for the $TiS_2$ molecule was observed

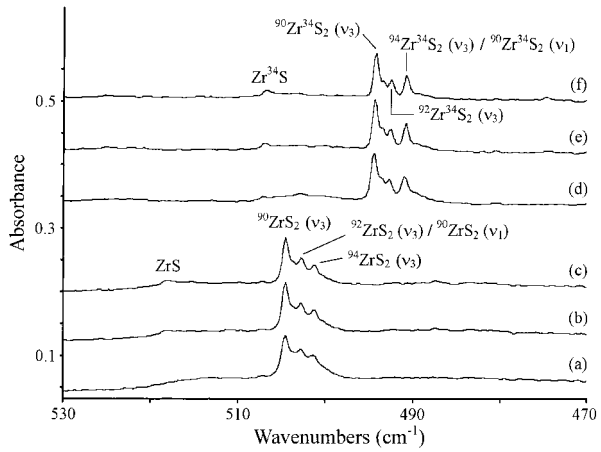


**Figure 3.** Infrared spectra in the 530−470 cm$^{-1}$ region for laser-ablated Zr co-deposited with discharged S in argon at 7 K. (a, b, c) $^{32}S$, (d, e, f) $^{34}S$. Spectra (a, d) are collected after sample deposition, (b, e) after 35 K annealing, (c, f) after 40 K annealing.

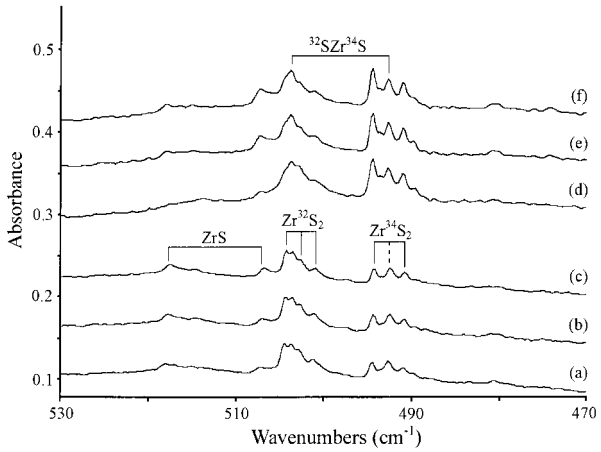


**Figure 4.** Infrared spectra in the 530−470 cm$^{-1}$ region for laser-ablated Zr co-deposited with discharged S in argon at 7 K. (a, b, c) 55/45 $^{32}S$ + $^{34}S$, (d, e, f) 35/65 $^{32}S$ + $^{34}S$. Spectra (a, d) are collected after sample deposition, (b, e) after 35 K annealing, (c, f) after 40 K annealing.

at 528.3 and 533.5 cm$^{-1}$ again in two matrix sites. In the mixed $^{32}S$ + $^{34}S$ experiment, the 528.3 cm$^{-1}$ band is split into a triplet absorption, which confirms the involvement of two equivalent sulfur atoms in this vibrational mode. Hence, we have identified $TiS_2$, and the observation of two Ti−S stretching modes shows that $TiS_2$ is a bent molecule.

The S−Ti−S valence angle can be computed using atomic masses and pairs of Ti and S isotopic $\nu_3$ frequencies assuming the force constant is isotopically invariant so that it cancels.[38,39] The upper and lower limits for the S−Ti−S bond angle are calculated as 114 ± 2° and 111 ± 2°, respectively.

*$ZrS_2$*. In the reaction between Zr and sulfur, the primary absorption feature after deposition was a three-band-set at 504.6, 502.9, and 501.3 cm$^{-1}$ (Figure 3a−c). This band-set showed little change on irradiation and sharpened on annealing to 35 and 40 K. Since the 40 K annealing (Figure 3c) provided the sharpest band profiles, the relative band height was measured then as 2.8:1.6:1. In the $^{34}S$ experiment, a better-resolved, corresponding three-band set was observed at 494.5, 492.8, and 491.0 cm$^{-1}$, with a slightly different relative height of 2.9:1:1.3 (Figure 3d−f). Zirconium has five natural isotopes: 51.45%, 11.27%, 17.17%, 17.33%, and 2.78% for mass = 90, 91, 92, 94, and 96, respectively.[37] The three-band-set observed in both $^{32}S$ and $^{34}S$ experiments are likely due to the isotopic splitting for a single Zr atom where the three most abundant isotopes, $^{90}Zr$, $^{92}Zr$, and $^{94}Zr$, have the relative abundance of approximately 3:1:1. Consequently, another absorption feature probably coincides at 502.9 cm$^{-1}$ in the $^{32}S$ sample and at 491.0 cm$^{-1}$ in the $^{34}S$ spectrum and skews the isotopic pattern of Zr. In the $^{34}S$ experiment, the bands were better resolved, and the $^{91}Zr$ band was almost resolved with appropriate relative absorption intensities (Figure 3d−f). The $^{32}S/^{34}S$ isotopic frequency ratios for these three bands are 1.0204, 1.0205, and 1.0210, respectively. The last ratio is different than the first two values, probably because the band center of the $^{34}S$ counterpart was shifted due to the coincidence with another absorption feature. These frequency ratios are considerably lower than the harmonic ratio for the diatomic ZrS molecule of 1.0224. For the coincident feature, the $^{32}S/^{34}S$ isotopic frequency ratio is 502.9/491.0 = 1.0242, which is higher than the diatomic frequency ratio. Similar to the $TiS_2$ molecule, the three-band set is assigned to the antisymmetric S−Zr−S stretching mode in the $ZrS_2$ molecule for the three most abundant zirconium isotopes. The coincident feature at 502.9 cm$^{-1}$ is the symmetric S−Zr−S stretching mode in $ZrS_2$ for the most abundant isotope $^{90}Zr$. The $\nu_1$ absorptions for other zirconium isotopes are even weaker, and also covered by other absorptions, and hence they are not identified. Two different $^{32}S$ + $^{34}S$ mixtures were employed for the zirconium reactions. Using a 55/45 mixture of $^{32}S$ + $^{34}S$ (Figure 4a−c), a new band at 503.8 cm$^{-1}$ was observed in addition to the six pure isotopic bands. The relative intensities for these six bands, however, are very different than the pure isotopic experiment. In the 35/65 $^{32}S$ + $^{34}S$ mixture (Figure 4d−f), all seven bands were again observed but with different relative intensities. The 503.8 cm$^{-1}$ band is assigned to the Zr−$^{32}S$ vibration in the $^{32}S$−Zr−$^{34}S$ molecule, and the Zr−$^{34}S$ vibration in the same molecule absorbs at 492.7 cm$^{-1}$, coincident with the antisymmetric $^{34}S$−$^{92}Zr$−$^{34}S$ stretching. Using $\nu_3$ frequencies for the $^{90}Zr^{32}S_2$ and $^{90}Zr^{34}S_2$ isotopic pairs (and for $^{92}Zr$) the upper limit for the S−Zr−S bond angle is calculated as 111 ± 2° and using $\nu_3$ frequencies for the $^{90}Zr^{32}S_2$ and $^{92}Zr^{32}S_2$ isotopic pairs (likewise for $^{34}S$) the lower limit is determined as 103 ± 2°.

To support further our spectroscopic assignment, a computer simulation was performed for the infrared spectra of the $ZrS_2$ stretching vibrations. The S−Zr−S bond angle was fixed at 107° (the median of the experimental upper and lower limits), and the high-frequency approximation, which assumes no interaction between $\nu_1$ and $\nu_2$ (bending) modes, was used. Figure 7a shows the $\nu_3$ spectra of both $Zr^{32}S_2$ and $Zr^{34}S_2$ for all zirconium isotopes, and in Figure 7b, the $\nu_1$ spectra of the same molecules are added to (a) with the assumption that $\nu_1$ is only one tenth as strong as $\nu_3$. Figure 7b simulates the experimental infrared spectra in Figure 3. Two mixed $^{32}S$ + $^{34}S$ spectra with different isotopic population ratios are plotted as Figure 7c and d, respectively, and each simulated the corresponding experimental infrared spectra in Figure 4. Overall, the simulated spectra match the experimental observations very well, and support the experimental assignments.

*$HfS_2$*. Similar to the $TiS_2$ and $ZrS_2$ molecules, the $HfS_2$ molecule was identified. In the $^{32}S$ experiment, a strong absorption at 483.2 cm$^{-1}$ and a weaker absorption at 492.2 cm$^{-1}$ tracked with each other throughout annealing and irradiation with relative absorption intensities of 10:1 (Figure 5). In the $^{34}S$ experiment, these bands shifted to 471.6 and 479.2 cm$^{-1}$ with $^{32}S/^{34}S$ isotopic frequency ratios of 1.0246 and 1.0271, respectively (Figure 6). The average of these two ratios, 1.0259, is close to the Hf $^{32}S$/Hf $^{34}S$ diatomic frequency ratio of 1.0260. In the mixed $^{32}S$ + $^{34}S$ experiment, these two bands clearly showed triplet splitting patterns with two new intermediate bands

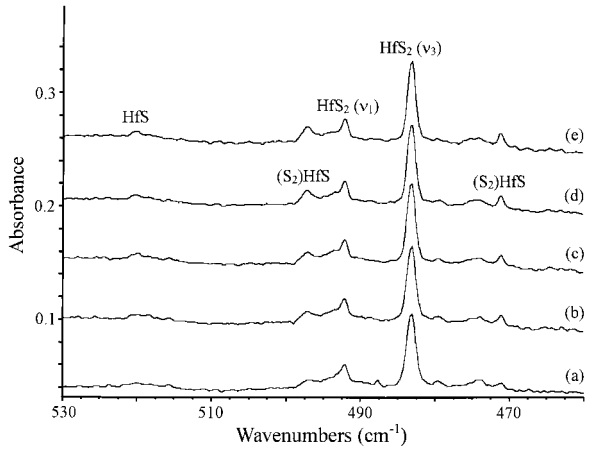


**Figure 5.** Infrared spectra in the 530−460 $cm^{-1}$ region for laser-ablated Hf co-deposited with discharged S in argon at 7 K. (a) Sample deposited for 40 min, (b) after 30 K annealing, (c) after $\lambda > 240$ nm irradiation, (d) after 35 K annealing, (e) after 40 K annealing.

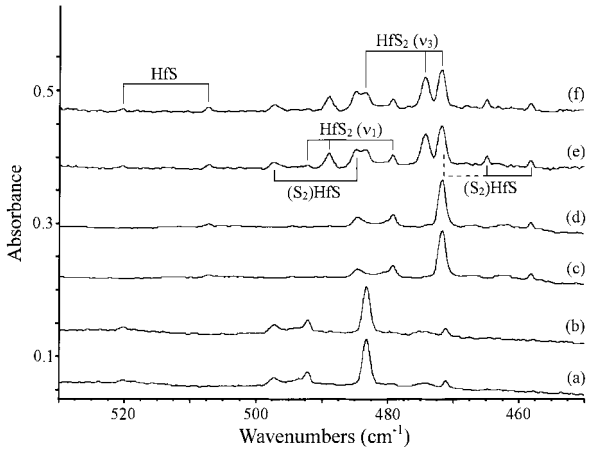


**Figure 6.** Infrared spectra in the 530−450 $cm^{-1}$ region for laser-ablated Hf co-deposited with discharged S in argon at 7 K. (a, b) $^{32}S$, (c, d) $^{34}S$, (e, f) 35/65 $^{32}S + {}^{34}S$ mixture. Spectra (a, c, e) are collected after 35 K annealing, (b, d, f) after 40 K annealing.

at 474.2 and 488.9 $cm^{-1}$, respectively. Hence, the 483.2 and 492.2 $cm^{-1}$ bands are assigned to the antisymmetric and symmetric S−Hf−S stretching modes in the $HfS_2$ molecule. The metal isotopic splitting patterns are not resolved for hafnium because the heavier apex atom introduces less isotopic shift. On the basis of the $\nu_3$ frequencies of $Hf\,^{32}S_2$ and $Hf\,^{34}S_2$, the upper limit[38,39] for the S−Hf−S bond angle is calculated as $112 \pm 2°$. If we take $ZrS_2$ as our model, where metal isotopic frequencies were employed to determine the angle lower limit, the experimental lower limit angle for $HfS_2$ will be on the order of 8° lower than the upper limit.

DFT calculations were performed on all three metal disulfides, and the results are summarized in Tables 3 and 4. Since all three metal atoms have electronic ground-state configurations of $d^2s^2$, the ground states for $MS_2$ are obviously singlets if no sulfur−sulfur bonds are involved. Calculations on cyclic $M(S_2)$ were also performed, and they are at least 40 kcal/mol higher than the open structures. The M−S bond lengths for the three $MS_2$ ground states are predicted as 2.086, 2.236, and 2.221 Å, and the S−M−S bond angles as 113.3°, 108.5°, and 109.5°, for M = Ti, Zr, and Hf, respectively. The bond lengths show the results of competition between shell-structure expansion and relativistic contraction,[40] as also found for the analogous oxides.[41] The DFT bond angles agree with the angles computed from experimental isotopic frequencies. Previous work has

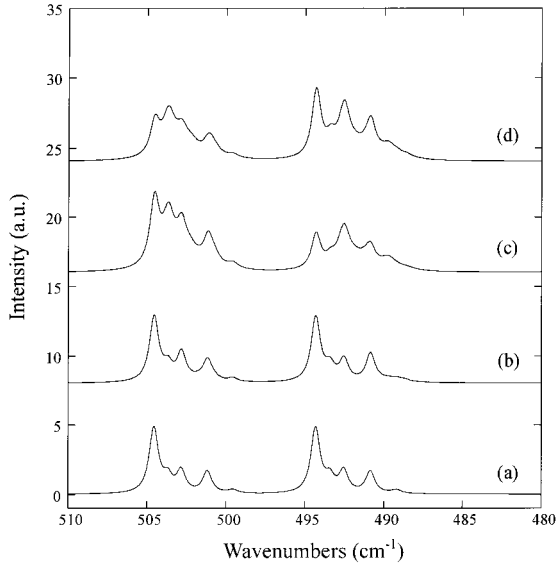


**Figure 7.** Simulations of the $ZrS_2$ vibrational spectra for zirconium natural isotopes. (a) Only the $\nu_3$ spectra for $Zr^{32}S_2$ and $Zr^{34}S_2$, (b) both the $\nu_3$ and $\nu_1$ spectra for $Zr^{32}S_2$ and $Zr^{34}S_2$, (c) mixed spectra for 55/45 $^{32}S + {}^{34}S$, (d) mixed spectra for 35/65 $^{32}S + {}^{34}S$.

**TABLE 2: Calculated Electronic State, Relative Energy, Geometry, Dipole Moment, and Frequencies for MS (M = Ti, Zr, Hf)**

| species | electronic state | relative energy [kcal/mol] | bond length [Å] | dipole moment [Debye] | frequency (intensity) [$cm^{-1}$ (km/mol)] |
|---|---|---|---|---|---|
| | | B3LYP | | | |
| TiS | $^3\Delta$ ($\delta^1\sigma^1$) | 0 | 2.086 | 5.579 | 567.1(78) |
| | $^3\Sigma^-$ ($\delta^2$) | +22.0 | 2.139 | 7.960 | 531.5(44) |
| | $^1\Sigma^+$ ($\sigma^2$) | +24.9 | 2.028 | 3.777 | 609.3(70) |
| ZrS | $^3\Delta$ ($\delta^1\sigma^1$) | 0 | 2.214 | 5.505 | 529.4(48) |
| | $^1\Sigma^+$ ($\sigma^2$) | +8.4 | 2.173 | 3.859 | 565.7(39) |
| | $^3\Sigma^-$ ($\delta^2$) | +24.4 | 2.252 | 7.704 | 492.0(54) |
| HfS | $^1\Sigma^+$ ($\sigma^2$) | 0 | 2.169 | 4.084 | 526.6(23) |
| | $^3\Delta$ ($\delta^1\sigma^1$) | +15.1 | 2.205 | 5.712 | 492.4(28) |
| | $^3\Sigma^-$ ($\delta^2$) | +60.3 | 2.241 | 7.249 | 453.9(25) |
| | | BPW91 | | | |
| ZrS | $^3\Delta$ ($\delta^1\sigma^1$) | 0 | 2.212 | 5.014 | 523.2(35) |
| | $^1\Sigma^+$ ($\sigma^2$) | +12.4 | 2.175 | 3.437 | 558.3(27) |
| | | MP2 | | | |
| ZrS | $^3\Delta$ ($\delta^1\sigma^1$) | 0 | 2.209 | 7.305 | 548.5(43) |
| | $^1\Sigma^+$ ($\sigma^2$) | +24.0 | 2.167 | 5.672 | 586.3(3) |

shown that the bond angle for the molecule is the average of upper and lower limits computed from pairs of terminal and apex isotopic $\nu_3$ frequencies for $C_{2v}$ molecules.[25,38] Hence, the valence angles for $TiS_2$, $ZrS_2$, and $HfS_2$, respectively, from experimental measurement are $113 \pm 4°$, $107 \pm 4°$, and $108 \pm 4°$.

The $MS_2$ vibrational frequencies are listed in Table 3. The $\nu_2$ bending modes for all three ground states are the weakest vibrations and below our detection limit, and hence they are not observed. Both $\nu_1$ and $\nu_3$ modes were observed for all three metals, and the calculated values agree quite well with the experimental results. In the case of $TiS_2$, the calculated frequencies are 3.4 and 5.4% too high, which is in agreement with comparison for inorganic molecules using the smaller 6-311G* basis set.[42] In the case of $ZrS_2$, the computed frequencies are 1.4 and 5.0% too high but for $HfS_2$ the frequencies are computed 1.9 and 0.3% too low, both using the LanL2DZ pseudopotential and basis set. The isotopic frequencies were also calculated, and they showed consistent agreement with experiment (Table 4). It is noteworthy that the calculation predicted two very close $\nu_1$ and $\nu_3$ frequencies for $ZrS_2$; $\nu_1$ is

calculated only 1.6 $cm^{-1}$ higher than $\nu_3$, whereas in the experiment, $\nu_3$ is 1.7 $cm^{-1}$ higher. Also in this molecule, the $\nu_1$ frequency is more than three times the value of the $\nu_2$ frequency, which validates the high-frequency approximation. Finally, the B3LYP functional, 6-311+G* basis, and LanL2DZ pseudopotential calculations show very good predictive power for group 4 disulfides. Similar agreement was found for group 5 sulfides.[36]

**MS (M = Ti, Zr, Hf).** *TiS.* The TiS system has been studied by many groups.[7−10] Recent high-resolution studies reported an $\omega_e$ value of 562.4 $cm^{-1}$, and a vibrational frequency of 558.3 $cm^{-1}$ for the $X^3\Delta$ state of the TiS molecule in the gas phase.[8] An earlier matrix isolation study using thermally evaporated Ti atom reactions with OCS produced a band at 552 $cm^{-1}$ in an OCS matrix and at 556 $cm^{-1}$ in an argon matrix, and these bands were assigned to the TiS fundamental.[20] In our Ti + S experiment (Figure 1), a weak band at 557.6 $cm^{-1}$ is very close to both gas-phase and earlier matrix values, and it is probably due to the TiS fundamental in the argon matrix. This band shifted to 529.7 $cm^{-1}$ in the $^{34}S$ experiment (Figure 2c,d), the isotopic frequency ratio of 1.0183 is close to the harmonic diatomic ratio of 1.0181. However, in the mixed $^{32}S + {}^{34}S$ experiment (Figure 2e,f), several weak, broad intermediate bands were observed. It is possible that the intermediate bands in the mixed isotopic experiment are due to absorptions other than TiS, nevertheless, the matrix assignment of 557.6 $cm^{-1}$ to the TiS fundamental is tentative.

In the complementary study using OCS as the sulfur source for reaction with laser-ablated Ti atoms, major product absorption bands were observed at 1868.1, 548.9, and 961.9 $cm^{-1}$. The former pair are probably the O−C and Ti−S stretching modes in the insertion product OCTiS, and the band at 961.9 $cm^{-1}$ is probably the O−Ti stretching mode in OTiCS. A detailed study of those products is beyond the scope of this investigation. We intended to find the TiS absorption in this OCS experiment, but the 557.6 $cm^{-1}$ band is unfortunately covered by nearby unknown complex absorptions, so no definitive conclusion can be drawn. It is noteworthy that the $TiS_2$ $\nu_3$ mode is observed in this OCS experiment, albeit very weakly ($A = 0.01$), in two matrix sites at 577.8 and 571.4 $cm^{-1}$, which are the same as in the sulfur discharge experiment.

*ZrS.* The first laboratory study of ZrS was performed by Simard et al. using laser-induced fluorescence.[11] In analogy with ZrO, the transition in the green region was labeled as $E^1\Sigma^+ - X^1\Sigma^+$. Later, Jonsson et al. systematically studied both singlet and triplet systems of ZrS, and reported $\omega_e$ values of 548.3 and 527.2 $cm^{-1}$, and vibrational frequencies of 545.4 and 524.5 $cm^{-1}$ for $X^1\Sigma^+$ and $a^3\Delta$ states, respectively.[12−14] To our knowledge, no experimental singlet−triplet energy separation has been reported.

In the current matrix experiment, a broad, weak band around 518 $cm^{-1}$ was observed on deposition, whereas no absorption was observed in the 545 $cm^{-1}$ region. This band sharpened on annealing, and was measured at 518.1 $cm^{-1}$ after 40 K annealing (Figure 3a−c). The band shifted to 506.8 $cm^{-1}$ in the $^{34}S$ experiment (Figure 3d−f) with a $^{32}S/^{34}S$ isotopic frequency ratio of 1.0221, which is very close to the harmonic diatomic ratio of 1.0224. In the mixed $^{32}S + {}^{34}S$ experiments (Figure 4), only doublets were found, which shows that only one sulfur atom is involved in the responsible absorber. We assign the 518.1 $cm^{-1}$ band to the vibration for triplet ZrS in the argon matrix. This matrix shift of 6.4 $cm^{-1}$ is smaller than the matrix shift (10.4 $cm^{-1}$) for ZrO at 958.6 $cm^{-1}$, but the percentage shifts are almost identical (1.2% for ZrS and 1.1% for ZrO).[41] Thus, it appears that the $^3\Delta$ state of ZrS is the lowest state in solid argon. Recall that high level theory predicted only 209 $cm^{-1}$ between the two states.[22]

*HfS.* The gas-phase study on HfS reported an $\omega_e$ value of 526.8 $cm^{-1}$, and a vibrational frequency of 524.4 $cm^{-1}$ for the $X^1\Sigma^+$ state.[16] In the current experiment, a weak band at 520.3 $cm^{-1}$ is assigned to the HfS fundamental in the argon matrix (Figure 5). This band red-shifted to 507.1 $cm^{-1}$ in the $^{34}S$ experiment (Figure 6c,d), and the $^{32}S/^{34}S$ isotopic frequency ratio of 1.0260 is the same as the harmonic diatomic ratio. In the mixed $^{32}S + {}^{34}S$ experiment (Figure 6e,f), this band split into a doublet, which confirms that only one sulfur atom is involved. The argon-matrix shift of 4.1 $cm^{-1}$ for HfS is smaller, both in absolute value and percentage, than the matrix shift (9.4 $cm^{-1}$) for HfO at 958.3 $cm^{-1}$.[41]

The bonding in transition metal monosulfides has been discussed in earlier studies.[21,43] It includes two components, the $\sigma$ bond between metal hybridized ds$\sigma$ and sulfur 3p$\sigma$ orbital electrons, and the $\pi$ bonds between metal d$\pi$ and sulfur p$\pi$ orbital electrons, and hence this bonding has a triple bond character. The metal d$\delta$ orbitals are nonbonding, and essentially do not effect bonding. The other hybridized ds$\sigma$ orbital is also nonbonding, but this orbital is very important in the bonding mechanism. The electrons in this orbital are polarized away from the sulfur atom, and to further reduce the $\sigma$ repulsion, the metal atom can undergo s to d electron promotion.

All three titanium group metal atoms have the ground-state valence electron configurations of $d^2s^2$. Excluding two electrons which are dedicated to M−S bonding, the ground states of metal monosulfides are determined by the configurations of two nonbonding electrons. DFT calculations were performed on all three of these systems for different electron configurations, and results are summarized in Table 2. From these calculations TiS and ZrS have $^3\Delta$ ground states with $\delta^1\sigma^1$ electron configurations, whereas HfS has the $^1\Sigma^+$ ground state with the $\sigma^2$ electron configuration. This difference could be due to the relativistic effect for the third-row transition metals,[40] which substantially stabilizes the 6s orbital of the hafnium atom, and subsequently two nonbonding electrons doubly occupy the $\sigma$ molecular orbital (mainly metal 6s character) in HfS. These current DFT/B3LYP ground states agree with gas-phase results only for TiS and HfS. As mentioned earlier in this paper, the gas-phase work reported a $^1\Sigma^+$ ground state for ZrS.[11,14,17] An earlier modified coupled-pair functional (MCPF) calculation on ZrS predicted the $^3\Delta$ state to be only 209 $cm^{-1}$ (less than 0.6 kcal/mol) higher than the $^1\Sigma^+$ state.[22] The current calculation puts the $^1\Sigma^+$ state at 8.4 kcal/mol higher than the $^3\Delta$ state. This energy difference could be due to inaccuracy in the DFT calculation. To further investigate this problem, additional DFT calculation using the BPW91 functional and the MP2 method were performed on ZrS. However, similar to the DFT/B3LYP calculation, the $^3\Delta$ ($\delta^1\sigma^1$) state is 12.4 and 24.0 kcal/mol lower than the $^1\Sigma^+$ ($\sigma^2$) state in the DFT/BPW91 and MP2 calculations, respectively (Table 2). Further calculations are necessary to clarify this difficult problem.

Vibrational analysis was performed on the metal monosulfides, and the results showed very good agreement with the experimental values (Table 2). In the case of ZrS, the 518.1 $cm^{-1}$ band is assigned to the fundamental of triplet ZrS trapped in the argon matrix, since it is close to the gas phase and calculated values for the triplet $^3\Delta$ state. A different ground state for ZrS in the gas phase and solid argon can be explained by the matrix effect. Because the triplet state has a larger dipole moment than the singlet state (Table 2), the stronger interaction

**TABLE 3: Calculated (DFT/B3LYP) Electronic State, Relative Energy, Geometry, and Frequencies for $MS_2$, (M = Ti, Zr, Hf) and $(S_2)HfS$**

| species | electronic state | relative energy [kcal/mol] | geometry [Å, deg] | frequency (intensity) [$cm^{-1}$ (km/mol)] |
|---|---|---|---|---|
| $TiS_2$ | $^1A_1$ | 0 | Ti−S: 2.086, ∠STiS: 113.3 | 597.6(187), 562.7(9), 173.0(2) |
| $Ti(S_2)$ | $^1A_1$ | +49.8 | Ti−S: 2.136, ∠STiS: 56.9 | 519.6(67), 386.6(4), 333.7(0) |
| $ZrS_2$ | $^1A_1$ | 0 | Zr−S: 2.236, ∠SZrS: 108.5 | 513.3(11), 511.7(146), 161.5(1) |
| $Zr(S_2)$ | $^1A_1$ | +53.8 | Zr−S: 2.387, ∠SZrS: 53.1 | 501.9(34), 359.5(8), 281.2(0) |
| $HfS_2$ | $^1A_1$ | 0 | Hf−S: 2.221, ∠SHfS: 109.5 | 490.5(6), 473.8(86), 151.3(1) |
| $Hf(S_2)$ | $^1A_1$ | +40.3 | Hf−S: 2.397, ∠SHfS: 53.9 | 495.2(12), 325.0(7), 280.5(0) |
| $(S_2)HfS'$ | $^1A'$ | 0 | S−Hf: 2.384, Hf−S′: 2.219, S−S: 2.220, ∠SHfS: 55.5, ∠SHfS′: 114.9 | 489.0(65), 448.4(30), 350.6(5), 293.9(18), 108.9(6), 82.8(5) |
| | $^1A_1$ | +13.8 | S−Hf: 2.402, Hf−S′: 2.244, S−S: 2.238, ∠SHfS′: 152.2 | 480.5(128), 434.0(14), 367.2(2), 264.2(7), 52.4i(19), 100.8i(41) |
| | $^3A''$ | +25.1 | S−Hf: 2.572, Hf−S′: 2.206, S−S: 2.038, ∠SHfS: 46.7, ∠SHfS′: 112.7 | 559.0(11), 486.5(25), 241.8(10), 216.5(2), 81.4(5), 66.5(3) |
| | $^3A_2$ | +33.1 | S−Hf: 2.631, Hf−S′: 2.214, S−S: 2.044, ∠SHfS′: 157.1 | 548.4(6), 496.3(95), 236.4(0), 230.6(29), 68.1i(8), 70.2i(13) |

between the triplet state and the host argon atoms lowers its energy more than the singlet state. It is noteworthy that the DFT/B3LYP calculated dipole moments for the $^3\Delta$ state TiS and $^1\Sigma^+$ state ZrS are close to experimental values (5.75 and 3.86 D, respectively).[19]

**$(S_2)HfS$.** In the Hf + S reaction, two associated bands at 497.2 and 471.1 $cm^{-1}$ were observed on deposition (Figure 5). These two bands almost doubled on 30 K annealing, showed little change on full-arc irradiation, and finally increased and sharpened slightly on 35 and 40 K annealings. The relative absorption intensity was measured after 40 K annealing as 1.8:1. In the $^{34}S$ experiment (Figure 6c,d), the 497.2 $cm^{-1}$ band red-shifted to 484.6 $cm^{-1}$, and the $^{32}S/^{34}S$ isotopic frequency ratio of 1.0260 is identical to the HfS fundamental. The 471.1 $cm^{-1}$ band shifted to 458.1 $cm^{-1}$, the isotopic frequency ratio of 1.0284 is even larger than that of the $HfS_2$ $\nu_1$ mode. In the $^{32}S + {}^{34}S$ experiment, the 497.2 $cm^{-1}$ band split into a doublet, and the 471.1 $cm^{-1}$ band split into a triplet with an intermediate band at 464.8 $cm^{-1}$. It is apparent that the 497.2 and 471.1 $cm^{-1}$ bands are due to vibrations involving one S atom and two equivalent S atoms, respectively. The molecule $(S_2)HfS$ is proposed, where the hafnium atom bonds to one sulfur atom and one $S_2$ unit. Two vibrations at 497.2 and 471.1 $cm^{-1}$ are the Hf−S stretching and $(S_2)$−Hf stretching modes.

DFT calculation on this $(S_2)HfS$ molecule was first performed on the planar $C_{2v}$ structure with a singlet spin state; however, imaginary frequencies were found (Table 3). Subsequent calculation was performed on a lower $C_s$ symmetry, where the S-atom deviates from the $(S_2)Hf$ plane. The lowest $^1A'$ state is 13.8 kcal/mol lower in energy than the $C_{2v}$ planar structure. More importantly, no imaginary vibrational frequencies were found. This bending can be understood from the bonding standpoint, since the linear structure would maximize the repulsion between the doubly occupied $\sigma$ orbital of HfS and the fully occupied $\pi$ orbitals of $S_2$. Calculations on the triplet spin state were also performed, and both lowest $C_{2v}$ and $C_s$ symmetry states are higher in energy than their respective singlet states (Table 3). The vibrational analysis on the ground $^1A'$ state predicted two strong modes at 489.0 and 448.4 $cm^{-1}$, with infrared intensities of 65 and 30 km/mol, respectively. These two modes are only 8.2 and 22.7 $cm^{-1}$ lower than two observed bands, and have similar relative intensities. Furthermore, the former mode is predicted as the terminal Hf−S stretching, and the latter is the $(S_2)Hf$ symmetric ring-stretching mode, and hence the isotopic splitting patterns in the mixed isotopic experiment are doublet and triplet, respectively. The calculated isotopic frequency ratios are listed in Table 4, which show excellent agreement with experimental values.

**TABLE 4: Comparison of Computed (B3LYP) and Experimental Metal−Sulfur Stretching Modes in $MS_2$ and $(S_2)HfS$**

| | | computed | | | experimental | | |
|---|---|---|---|---|---|---|---|
| species | mode | $M^{32}S_2$ | $M^{34}S_2$ | $R$(32/34) | $M^{32}S_2$ | $M^{34}S_2$ | $R$(32/34) |
| $TiS_2$ | $a_1$ | 562.7 | 551.5 | 1.0203 | 528.3 | 517.8 | 1.0203 |
| | $b_2$ | 597.6 | 588.4 | 1.0156 | 571.4 | 562.6 | 1.0156 |
| $ZrS_2$ | $a_1$ | 513.3 | 501.4 | 1.0237 | 502.9 | 491.0 | 1.0242 |
| | $b_2$ | 511.7 | 501.3 | 1.0207 | 504.6 | 494.5 | 1.0204 |
| $HfS_2$ | $a_1$ | 490.5 | 477.6 | 1.0270 | 492.2 | 479.2 | 1.0271 |
| | $b_2$ | 473.8 | 462.4 | 1.0247 | 483.2 | 471.6 | 1.0246 |
| $(S_2)HfS$ | a′ | 489.0 | 476.6 | 1.0260 | 497.2 | 484.6 | 1.0260 |
| | a′ | 448.4 | 436.0 | 1.0284 | 471.1 | 458.1 | 1.0284 |

**Other Absorptions.** In the titanium experiment, a broad, weak band observed at 539.2 $cm^{-1}$ shifted to 529.7 $cm^{-1}$ in the $^{34}S$ experiment. In the mixed $^{32}S + {}^{34}S$ experiment, the band apparently split into a doublet. This band is too low to assign to the TiS fundamental in the argon matrix. We tentatively assign it as a titanium cluster sulfide, $Ti_xS$, where $x$ likely equals 2.

**Reaction Mechanisms.** Possible reactions for product formation, along with zero-point-energy corrected relative energy changes calculated by DFT/B3LYP are:

$$M + S \rightarrow MS \quad (\Delta E = -108, -125, -131 \text{ kcal/mol for Ti, Zr, Hf}) \quad (1)$$

$$M + S_2 \rightarrow MS + S \quad (\Delta E = -15, -32, -38 \text{ kcal/mol for Ti, Zr, Hf}) \quad (2)$$

$$M + S_3 \rightarrow MS + S_2 \quad (\Delta E = -63, -80, -86 \text{ kcal/mol for Ti, Zr, Hf}) \quad (3)$$

$$M + S_2 \rightarrow MS_2 \quad (\Delta E = -11, -139, -134 \text{ kcal/mol for Ti, Zr, Hf}) \quad (4)$$

$$M + S_3 \rightarrow MS_2 + S \quad (\Delta E = -6, -94, -89 \text{ kcal/mol for Ti, Zr, Hf}) \quad (5)$$

$$Hf + S_3 \rightarrow (S_2)HfS \quad (\Delta E = -166 \text{ kcal/mol}) \quad (6)$$

$$HfS + S_2 \rightarrow (S_2)HfS \quad (\Delta E = -80 \text{ kcal/mol}) \quad (7)$$

The $\Delta E$ values for reaction 1 are actually $-D_0$ values for the MS molecules. Only $D_0$ for TiS has been measured experimentally,[43] and our calculated value agrees with the reported value of 109 kcal/mol.

In the current experiment, the dominant processes for the formation of MS and $MS_2$ cannot be determined. Although all five proposed reactions are thermodynamically favored for all three metals, no apparent increase of the MS and $MS_2$ bands was observed during annealing and irradiation cycles in the matrixes. Metal sulfides are formed only during the laser-ablation processes when the ablated metal atoms provide sufficient excess energy[44] to overcome the reaction barriers. This result suggests that the formation of MS and $MS_2$ requires activation energy. Reactions 2 and 4 are probably most important as $S_2$ is expected to be the major sulfur reagent, although its concentration could not be measured, and $MS_2$ is the dominant product.

Reactions 6 and 7 provide two possible pathways to form the product $(S_2)$HfS. During sample deposition, the reaction between laser-ablated Hf atom and $S_3$ forms an initial adduct, which rearranges in the argon matrix to give $(S_2)$HfS. Reaction 7 likely happens during the annealing process where excess $S_2$ in the argon matrix reacts with HfS to form $(S_2)$HfS.

## V. Conclusions

Laser-ablated titanium, zirconium, and hafnium atoms react with discharged sulfur vapor during co-condensation in excess argon. The primary reaction products $MS_2$ are identified here for the first time, and the $\nu_1$ and $\nu_3$ modes for M = Ti, Zr, and Hf absorb at 533.5 and 577.8 $cm^{-1}$, 502.9 and 504.6 $cm^{-1}$, and 492.2 and 483.2 $cm^{-1}$, respectively. On the basis of the isotopic frequencies of the $\nu_3$ modes, the bond angles of the $C_{2v}$ molecules $TiS_2$, $ZrS_2$, and $HfS_2$ are determined as $113 \pm 4°$, $107 \pm 4°$, and $108 \pm 4°$. Successful angle determinations from isotopic $\nu_3$ frequencies have been made for sulfur-bearing molecules.[25,36,38] Evidence for metal monosulfides is presented: ZrS and HfS absorb at 518.1 and 520.3 $cm^{-1}$, respectively, whereas a weak absorption at 557.6 $cm^{-1}$ is tentatively assigned to the TiS fundamental.

The trend in stretching frequencies observed here for $TiS_2$, $ZrS_2$, and $HfS_2$ (577.8, 533.5 $cm^{-1}$ to 504.6, 502.9 $cm^{-1}$ to 483.2, 492.2 $cm^{-1}$) is analogous to that observed for $TiO_2$, $ZrO_2$, and $HfO_2$ (946.9, 917.1 $cm^{-1}$ to 884.3, 818.0 $cm^{-1}$ to 883.4, 814.0 $cm^{-1}$).[41] The decrease in frequencies from Ti to Zr for shell expansion is not matched from Zr to Hf because of relativistic contraction.[40] The group 4 disulfide molecule stretching frequencies are 56−63% of their dioxide counterparts. Furthermore, the group 4 dioxide and disulfide bond angles are the same for common transition metals within experimental error. A like similarity has been found for the group 5 dioxide and disulfide molecules.[36]

Straightforward DFT/B3LYP calculations on the metal disulfides find $^1A_1$ ground states, with bond angles of 113.3°, 108.5°, and 109.5°, for $TiS_2$, $ZrS_2$, and $HfS_2$, respectively, in agreement with the above experimental determinations. Our DFT calculations also predict $^3\Delta$ ground states for TiS and ZrS, but the $^1\Sigma^+$ ground state for HfS. Finally, DFT calculations give isotopic frequencies in excellent agreement with the observed values, which supports the present product identifications and the future predictive power of DFT calculations for transition metal sulfides.

**Acknowledgment.** The authors gratefully acknowledge National Science Foundation support from Grant CHE 00-78836.

## References and Notes

(1) *Transition Metal Sulfur Chemistry, Biological and Industrial Significance*; Stiefel, E. I., Matsumoto, K., Eds.; American Chemical Society: Washington, DC, 1997.
(2) *Transition Metal Sulphides, Chemistry and Catalysis*; Weber, T., Prins, R., van Santen, R. A., Eds.; NATO ASI Series; Kluwer Academic Publishers: The Netherlands, 1998.
(3) Pecoraro, T. A.; Chianelli, R. R. *J. Catal.* **1981**, *67*, 430. Chianelli, R. R.; Daage, M.; Ledoux, M. J. *Adv. Catal.* **1994**, *40*, 177.
(4) Sweeney, Z. K.; Polse, J. L.; Bergman, R. G.; Andersen, R. A. *Organometallics* **1999**, *18*, 5502.
(5) Jonsson, J.; Lindgren, B.; Taklif, A. G. *Astron. Astrophys.* **1991**, *246*, L67. Jonsson, J.; Launila, O.; Lindgren, B. *Mon. Not. R. Astron. Soc.* **1992**, *258*, 49.
(6) Verma, A. K.; Chou, J.-H.; Rauchfuss, T. B. *Inorg. Chem.* **1998**, 5960.
(7) Clements, R. M.; Barrow, R. F. *Trans. Faraday Soc.* **1969**, *65*, 1163.
(8) Jonsson, J.; Launila, O. *Mol. Phys.* **1993**, *79*, 95.
(9) Ran, Q.; Tam, W. S.; Ma, C. S.; Cheung, A. S. C. *J. Mol. Spectrosc.* **1999**, *198*, 175.
(10) Cheung, A. S. C.; Ran, Q.; Tam, W. S.; Ma, C. S. *J. Mol. Spectrosc.* **2000**, *203*, 96.
(11) Simard, B.; Mitchell, S. A.; Hackett, P. A. *J. Chem. Phys.* **1988**, *89*, 1899.
(12) Jonsson, J. *J. Mol. Spectrosc.* **1995**, *169*, 18.
(13) Jonsson, J.; Lindgren, B. *J. Mol. Spectrosc.* **1995**, *169*, 30.
(14) Jonsson, J.; Wallin, S.; Lindgren, B. *J. Mol. Spectrosc.* **1998**, *192*, 198.
(15) Jonsson, J.; Edvinsson, G.; Taklif, A. G. *Phys. Scr.* **1994**, *50*, 661.
(16) Launila, O.; Jonsson, J.; Edvinsson, G.; Taklif, A. G. *J. Mol. Spectrosc.* **1996**, *177*, 221.
(17) Beaton, S. A.; Gerry, M. C. L. *J. Chem. Phys.* **1999**, *110*, 10715.
(18) Steimle, T. C.; Costen, M. L.; Hall, G. E.; Sears, T. J. *Chem. Phys. Lett.* **2000**, *319*, 363.
(19) Bousquet, R. R.; Namiki, K. C.; Steimle, T. C. *J. Chem. Phys.* **2000**, *113*, 1566.
(20) DeVore, T. C.; Franzen, H. F. *High Temp. Sci.* **1975**, *7*, 220.
(21) Bauschlicher, C. W., Jr.; Maitre, P. *Theor. Chim. Acta* **1995**, *90*, 189.
(22) Langhoff, S. R.; Bauschlicher, C. W., Jr. *J. Chem. Phys.* **1988**, *89*, 2160.
(23) Dance, I. G.; Fisher, K. J.; Willett, G. D. *Inorg. Chem.* **1996**, *35*, 4177.
(24) Kretzschmar, I.; Schröder, D.; Schwarz, H.; Rue, C.; Armentrout, P. B. *J. Phys. Chem. A* **2000**, *104*, 5046.
(25) Brabson, G. D.; Mielke, Z.; Andrews, L. *J. Phys. Chem.* **1991**, *95*, 79.
(26) Long, S. R.; Pimentel, G. C. *J. Chem. Phys.* **1977**, *66*, 2219.
(27) Smardzewski, R. R. *J. Chem. Phys.* **1978**, *68*, 2878.
(28) Burkholder, T. R.; Andrews, L. *J. Chem. Phys.* **1991**, *95*, 8697.
(29) Hassanzadeh, P.; Andrews, L. *J. Phys. Chem.* **1992**, *96*, 9177.
(30) Frisch, M. J.; Trucks, G. W.; Schlegel, H. B.; Scuseria, G. E.; Robb, M. A.; Cheeseman, J. R.; Zakrzewski, J. A.; Montgomery, J. A.; Stratmann, R. E.; Burant, J. C.; Dapprich, S.; Millam, J. M.; Daniels, A. D.; Kudin, K. N.; Strain, M. C.; Farkas, O.; Tomasi, J.; Barone, V.; Cossi, M.; Cammi, R.; Mennucci, B.; Pomelli, C.; Adamo, C.; Clifford, S.; Ochterski, J.; Petersson, G. A.; Ayala, P. Y.; Cui, Q.; Morokuma, K.; Malick, D. K.; Rabuck, A. D.; Raghavachari, K.; Foresman, J. B.; Cioslowki, J.; Ortiz, J. V.; Stefanov, B. B.; Liu, G.; Liashenko, A.; Piskorz, P.; Komaromi, I.; Gomperts, R.; Martin, R. L.; Fox, D. J.; Keith, T.; Al-Laham, M. A.; Peng, C. Y.; Nanayakkara, A.; Gonzalez, C.; Challacombe, M.; Gill, P. M. W.; Johnson, B. G.; Chen, W.; Wong, M. W.; Andres, J. L.; Head-Gordon, M.; Replogle, E. S.; Pople, J. A. *Gaussian 98*, revision A.1.; Gaussian, Inc.: Pittsburgh, PA, 1998.
(31) Lee, C.; Yang, E.; Parr, R. G. *Phys. Rev. B* **1988**, *37*, 785.
(32) Perdew, J. P.; Wang, Y. *Phys. Rev. B* **1992**, *45*, 13244.
(33) Frisch, M. J.; Head-Gordon, M.; Pople, J. A. *Chem. Phys. Lett.* **1990**, *166*, 281.
(34) McLean, A. D.; Chandler, G. S. *J. Chem. Phys.* **1980**, *72*, 5639. Wachters, A. J. H. *J. Chem. Phys.* **1970**, *52*, 1033. Hay, P. J. *J. Chem. Phys.* **1977**, *66*, 4377. Raghavachari, K.; Trucks, G. W. *J. Chem. Phys.* **1989**, *91*, 1062.
(35) Hay, P. J.; Wadt, W. R. *J. Chem. Phys.* **1985**, *82*, 270. Wadt, W. R.; Hay, P. J. *J. Chem. Phys.* **1985**, *82*, 284. Hay, P. J.; Wadt, W. R. *J. Chem. Phys.* **1985**, *82*, 299.
(36) Liang, B.; Andrews, L. *J. Phys. Chem. A* **2002**, *106*, 3738 (V, Nb, Ta + $S_2$).
(37) *CRC Handbook of Chemistry and Physics*; CRC Press: Boca Raton, FL, 1985.
(38) Allavena, M.; Rysnik, R.; White, D.; Calder, V.; Mann, D. E. *J. Chem. Phys.* **1969**, *50*, 3399.
(39) Andrews, L. *J. Electron Spectrosc. Relat. Phenom.* **1998**, *97*, 63.
(40) Pyykkö, P. *Chem. Rev.* **1988**, *88*, 563.
(41) Chertihin, G. V.; Andrews, L. *J. Phys. Chem.* **1995**, *99*, 6356.
(42) Bytheway, I.; Wong, M. W. *Chem. Phys. Lett.* **1998**, *282*, 219.
(43) Huber, K. P.; Herzberg, G. *Constants of Diatomic Molecules*; Van Nostrand Reinhold: New York, 1979.
(44) Kang, H.; Beauchamp, J. L. *J. Phys. Chem.* **1985**, *89*, 3364.